University of Reading

The potential of machine learning to predict melting response time of phase change materials in triplex-tube latent thermal energy storage systems

Article

Published Version

Creative Commons: Attribution 4.0 (CC-BY)

Open Access

Yan, P., Wen, C. ORCID: https://orcid.org/0000-0002-4445-1589, Ding, H., Wang, X. and Yang, Y. (2025) The potential of machine learning to predict melting response time of phase change materials in triplex-tube latent thermal energy storage systems. Applied Energy, 390. 125863. ISSN 1872-9118 doi: 10.1016/j.apenergy.2025.125863 Available at https://centaur.reading.ac.uk/122526/

It is advisable to refer to the publisher's version if you intend to cite from the work. See Guidance on citing.

To link to this article DOI: http://dx.doi.org/10.1016/j.apenergy.2025.125863

Publisher: Elsevier

All outputs in CentAUR are protected by Intellectual Property Rights law, including copyright law. Copyright and IPR is retained by the creators or other copyright holders. Terms and conditions for use of this material are defined in the End User Agreement.

University of Reading

www.reading.ac.uk/centaur

CentAUR

Central Archive at the University of Reading

Reading's research outputs online

Applied Energy 390 (2025) 125863

Contents lists available at ScienceDirect

Applied Energy

journal homepage: www.elsevier.com/locate/apenergy

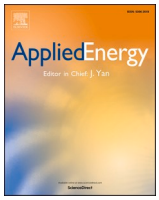

The potential of machine learning to predict melting response time of phase change materials in triplex-tube latent thermal energy storage systems☆

Peiliang Yan [a], Chuang Wen [b,*], Hongbing Ding [c], Xuehui Wang [d], Yan Yang [e,*]

[a] School of Energy and Power Engineering, Beihang University, Beijing 100191, China
[b] School of the Built Environment, University of Reading, Reading RG6 6AH, United Kingdom
[c] School of Electrical and Information Engineering, Tianjin University, Tianjin 300072, China
[d] School of Mechanical & Materials Engineering, University College Dublin, Dublin D04 V1W8, Ireland
[e] Faculty of Environment, Science and Economy, University of Exeter, Exeter EX4 4QF, United Kingdom

HIGHLIGHTS

- Y-shaped fins to enhance phase change material charging performance in latent thermal energy storage systems.
- Predicting melting response time using four machine learning methods.
- Evaluation of model performance using mean square error and coefficient of determination.
- Conducted Feature importance evaluation to guide fin improvements.

ARTICLE INFO

Keywords:
Phase change material
Thermal energy storage
Machine learning
Melting response time
XGBoost algorithm

ABSTRACT

Accurate prediction of the melting response time is vital for optimizing thermal energy storage systems, which play a key role in addressing the temporal mismatch between thermal energy demand and supply in the built environment. This study aims to quantitatively predict the melting response time of a novel triplex-tube thermal energy storage system incorporating phase change materials and Y-shaped fins to enhance heat transfer. A numerical model based on the enthalpy-porosity method was developed to simulate the melting process, resulting in a dataset comprising 60 cases with melting response times ranging from 15 to 45 min under varying design and operational conditions. The key parameters investigated include fin angle (10°–30°), fin width (5–15 mm), and heat transfer fluid temperature (60 °C–80 °C). Prior to model development, variable independence was validated to ensure robust predictions. Four machine learning algorithms—polynomial regression, support vector regression, random forest regression, and extreme gradient boosting (XGBoost)—were employed, with hyperparameter optimization performed using a Bayesian approach. The XGBoost model demonstrated superior predictive capability, achieving an accuracy of 92 %. Feature importance analysis revealed that fin width and heat transfer fluid temperature were the dominant factors, contributing 51 % and 47 % to the prediction variance, respectively, whereas fin angle had a marginal influence of 2 %. This work provides a novel application of machine learning techniques to the design and optimization of thermal energy storage systems, offering valuable insights into improving their melting performance and operational efficiency.

1. Introduction

In the last century, the global average temperature has risen significantly, primarily due to industrialization. According to the 6th Assessment Report from the Intergovernmental Panel on Climate Change (IPCC, 2023), global surface temperatures have increased by 1.09 °C [1]. This rise in temperature poses serious challenges, prompting various industries to recognize the urgent need to adopt renewable energy sources to reduce carbon emissions [2–4]. For instance, many modern urban buildings are now using solar collectors to supply heating [5]. However, a major issue is that peak heating demand often does not align with when solar energy is available [6]. To address this mismatch, the main solutions involve electrical options and thermal energy storage

☆ This article is part of a Special issue entitled: 'Decarbonize the Industry(Zishuai Bill Zhang)' published in Applied Energy.

* Corresponding authors.
E-mail addresses: c.wen@reading.ac.uk (C. Wen), y.yang7@exeter.ac.uk (Y. Yang).

https://doi.org/10.1016/j.apenergy.2025.125863
Received 26 January 2025; Received in revised form 26 March 2025; Accepted 3 April 2025
Available online 10 April 2025
0306-2619/© 2025 The Authors. Published by Elsevier Ltd. This is an open access article under the CC BY license (http://creativecommons.org/licenses/by/4.0/).

Nomenclature

English symbols

C	model constants
c	heat capacity [J/kg·K]
g	gravity constant [m/s^2]
H	latent heat [J/kg]
k	thermal conductivity [W/m·K]
p	pressure [Pa]
S	source term
T	temperature [K]
t	time [s]
u	fluid velocity in x direction [m/s]
v	fluid velocity in y direction [m/s]

Greek symbols

β	thermal expansion coefficient [1/K]
ε	model constants
θ	fin angle [°]
λ	local liquid fraction
μ	dynamic viscosity [Pa·s]
ρ	density [kg/m^3]

Subscripts

l	liquid
m	melting
p	constant pressure
s	solid
ref	reference

Abbreviations

HTF	heat transfer fluid
MSE	mean square error
PCM	phase change material
PR	polynomial regression
R^2	coefficient of determination
RFR	random forest regression
SVR	support vector regression
TES	thermal energy storage
XGboost	extreme gradient boosting

(TES) [7]. While electrical systems can provide flexibility, they often rely on fossil fuels, leading to higher carbon emissions. In contrast, TES systems store solar energy as heat, resulting in lower emissions and a more sustainable approach to achieving carbon neutrality in the built environment.

TES can be divided into three types: sensible, latent, and thermochemical energy storage [8]. Latent heat storage, which uses phase change materials (PCMs), has gained considerable interest in recent years [9]. This technology allows for the efficient storage and release of energy at nearly constant temperatures while maintaining a high energy storage density [10]. Its applications extend across various fields, such as the food industry [11], battery thermal management [12], distributed heat supply systems [13], solar thermal supply [14] and other fields [15–17].

A common component of latent heat storage systems is the triplex-tube latent thermal energy exchanger. This system consists of three tubes arranged to form three channels: the inner and outer channels are filled with heat transfer fluid (HTF), while the middle channel contains the PCM [18]. During the charging process, the PCM in the middle channel absorbs heat and begins to melt, effectively storing energy. When there is a demand for heating, the stored thermal energy can be released back into the system, providing a reliable source of heat even when solar energy is not available.

However, the poor thermal conductivity of PCMs results in a slow rate of energy release, which limits their application [19]. Therefore, researchers have conducted some studies on the enhancement of melting speed in PCM. Common heat transfer enhancement techniques include inserting fins [20], adding nanoparticles [21], etc. While these methods slightly reduce the volume proportion of PCM in the middle channel of a triplex-tube latent thermal energy exchanger, they can significantly improve the heat transfer rate and yield better results. Importantly, the chemical stability of PCMs remains intact, even after many charging cycles [22].

Factors such as fin length [23], initial temperature [24], and many other parameters can greatly affect the heat transfer performance of triplex-tube latent thermal energy storage systems. It is essential to understand how different parameters influence the heat transfer effect when designing new systems. To quantify these impacts, researchers have conducted numerous studies.

Direct measurement of the melt time of TES systems using experimental method is an accurate way to obtain heat transfer performance. In contrast, more researchers are using numerical simulation methods to obtain melt time because of the high cost of manufacturing components for different experiments in different conditions. In triplex-tube TES systems, researchers have designed a variety of fins [25–27] and tested them using simulation methods to reduce costs and enhance efficiency.

To accelerate the optimization process, researchers use faster predictive models to replace time-consuming simulation methods. One approach is the empirical formula method, where researchers derive data through experimentation or simulation and then fit it into mathematical formulas. Rieger was among the first to summarize empirical formulas related to the heat transfer performance of phase change materials, providing empirical formulas for the Nusselt number in relation to the Rayleigh number for a PCM in a heated cylinder [28]. Wang summarized empirical formulas for the melting behavior of a heated vertical wall in a rectangular enclosure [29]. Assis presented an empirical formula for the melting of PCM inside a spherical shell [30]. Chabot et al. described the relationship between the solid crust dimension of periodically heated horizontal tubes and three dimensionless numbers: the Prandtl number, Stefan number, and Rayleigh number [31]. Despite these contributions, the empirical formula method has notable shortcomings. The equations take various forms, often failing to accurately represent the actual relationships between variables, making them applicable only to specific scenarios. When attempting to extend these formulas to new situations, their forms may need adjustment or entirely new formulas may have to be developed. Additionally, the prediction accuracy of these formulas can be limited, leading to significant errors under certain conditions. These limitations have driven researchers to seek new prediction methods.

Machine learning has emerged as a powerful prediction tool in recent decades, attracting the interest of researchers across various industries [32–34]. In the field of phase change material based TES system researches, Ermis et al. used artificial neural networks (ANN) to predict the thermal storage capacity of a PCM-based finned tube thermal storage system [35]. Fini et al. applied the ANN approach to identify optimal working conditions for PCM-based battery cooling [36]. Walker et al. developed an algorithm that predicts the remaining time for a PCM to reach a target melting fraction in real time for an electronic device cooling system, also using an ANN [37]. These examples demonstrate that machine learning methods for predicting heat transfer performance related to PCMs offer significant advantages.

For predicting the melting time of the TES system, traditional methods have been the mainstream approach, as previously discussed, and these methods have been widely applied across different TES

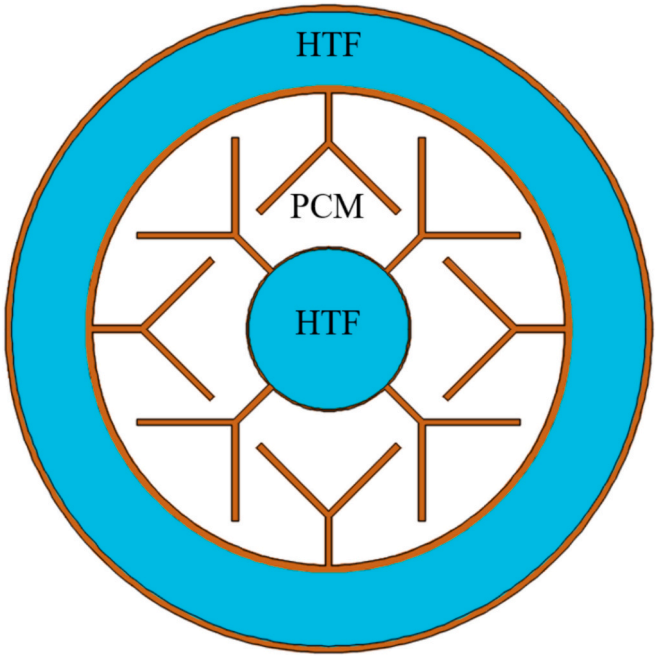

Fig. 1. Cross-section of the object TES system.

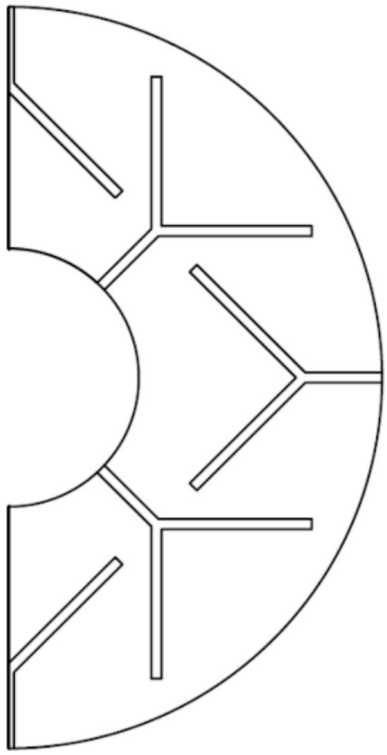

Fig. 2. The computational domain.

systems. However, in recent years, data-driven machine learning techniques have gained popularity for their ability to quickly predict melting outcomes, thus circumventing the lengthy numerical simulation processes. To create meta-models of the first-principle simulation model for this scenario, it is essential to explore various types of machine learning models in order to identify an effective model for predicting melting time.

In our previous work, we established a triplex-tube PCM-TES system featuring novel Y-shaped fins and qualitatively analyzed the effects of various parameters [38]. Building on these findings, the present study aims to enhance the prediction of melting response time in this triplex-tube latent thermal energy storage (TES) system using machine learning techniques. To achieve this aim, the following objectives have been identified: developing predictive models, evaluating their performance, conducting sensitivity analysis, optimizing hyperparameters, and providing design guidelines.

Table 1
The explanation and value of the parameters.

Parameters	Unit	Explanation	Values
Fin width	mm	Fin short side dimensions	0.5,1,1.5,2
Fin angle	°	Y-shaped fin branch angle	30,60,90
HTF temperature	K	HTF temperature during discharging energy process	363 , 365.5 , 368 , 370.5 , 373

Table 2
The explanation and value of the parameters.

Property	RT82	Copper
ρ [kg/m^3]	770	8920
c_p [J/kg·K]	2000	381
k [W/m·K]	0.2	387.6
μ [Pa·s]	0.03499	–
H [J/kg]	176,000	–
T_s [K]	350.15	–
T_l [K]	358.15	–
β [1/K]	0.001	–

2. Dataset

2.1. TES system

The research object of the study is a triplex-tube novel thermal energy storage system. PCMs are used to store thermal energy, with Y-shaped fins for heat transfer enhancement, which has a cross-sectional structure as shown in Fig. 1. The outer diameters of the three concentric copper tubes from the outside to the inside are 200 mm, 150 mm and 50.8 mm respectively, and the wall thicknesses are 2 mm, 2 mm and 1.2 mm respectively. The fins are attached to the inner and middle tubes of the middle annular region and staggered, respectively. The total cross-sectional area of the Y-fin is fixed as 2 % of the cross-sectional area of the system, and the length of the branch fins is twice the length of the root fin, making the structure of the Y-fin in this case controlled by three parameters (See Fig. 2). The explanation of the parameters and their values are given in Table 1. In this study, RT82 was used as the PCM and copper was used as the material for the fins as well as the tubes, the physical properties of which are shown in Table 2.

2.2. Simulation method

The dataset for this study was obtained by the same numerical simulation method as in the previous work [38]. The enthalpy-porosity method is a commonly used approach for simulating solid-liquid phase changes [39]. The enthalpy-porosity model treats the mushy zone as a porous medium when the solids are melting and equates the liquid phase volume fraction to the porosity of the porous medium to represent the melting process. The model is controlled by:

Continuity equation:

$$\frac{\partial \rho}{\partial t}+\frac{\partial(\rho u)}{\partial x}+\frac{\partial(\rho v)}{\partial y}=0 \tag{1}$$

The momentum sink caused by solidification are expressed by source terms [40] in the enthalpy-porosity model, and the momentum equations are:

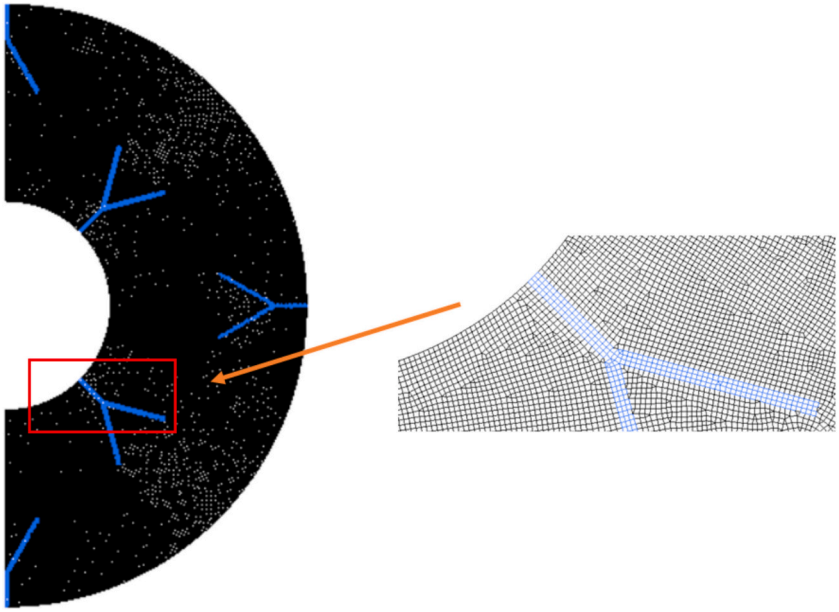

Fig. 3. The grid distribution.

$$\frac{\partial(\rho u)}{\partial t}+\frac{\partial(\rho uu)}{\partial x}+\frac{\partial(\rho vu)}{\partial y}=-\frac{\partial p}{\partial x}+\frac{\partial}{\partial x}\left(\mu\frac{\partial u}{\partial x}\right)+\frac{\partial}{\partial y}\left(\mu\frac{\partial u}{\partial y}\right)+uA \tag{2}$$

$$\frac{\partial(\rho v)}{\partial t}+\frac{\partial(\rho uv)}{\partial x}+\frac{\partial(\rho vv)}{\partial y}=-\frac{\partial p}{\partial y}+\frac{\partial}{\partial x}\left(\mu\frac{\partial v}{\partial x}\right)+\frac{\partial}{\partial y}\left(\mu\frac{\partial v}{\partial y}\right)+vA+\rho g\beta(T-T_m) \tag{3}$$

A in the source terms can be computed using the porosity function:

$$A=-C\frac{(1-\lambda)^2}{\lambda^3+\varepsilon} \tag{4}$$

λ is the liquid fraction of the PCM throughout this study, which is calculated as

$$\lambda=\begin{cases}0, & T<T_s\\ \dfrac{T-T_s}{T_l-T_s}, & T_s<T<T_l\\ 1, & T>T_l\end{cases} \tag{5}$$

The mushy zone constant C is a key element of the Carman-Kozeny equation, which adds a damping term to the momentum equation, modeling fluid flow in the mushy zone as flow through a porous medium [41]. The constant can be obtained through empirical correlation Eqs. [42]. For most calculations, the recommended values are between 10^4 and 10^7. After our adjustments, this model selects $C=10^6$. ε is simply an arbitrary minimum protection against a denominator of zero, which is set to be ε = 0.001.

Energy equation with external heat source term:

$$\frac{\partial(\rho h)}{\partial t}+\frac{\partial(\rho uh)}{\partial x}+\frac{\partial(\rho vh)}{\partial y}=\frac{\partial}{\partial x}\left(k\frac{\partial T}{\partial x}\right)+\frac{\partial}{\partial y}\left(k\frac{\partial T}{\partial y}\right)+S \tag{6}$$

h is defined as

$$h=\begin{cases}\displaystyle\int_{T_{ref}}^{T}c_p dT, & T<T_s\\ \displaystyle\int_{T_{ref}}^{T_s}c_p dT+\lambda H, & T_s<T<T_l\\ \displaystyle\int_{T_{ref}}^{T_s}c_p dT+H+\int_{T_l}^{T}c_p dT, & T>T_l\end{cases} \tag{7}$$

T could be calculated as

$$T=\lambda(T_l-T_s)+T_s \tag{8}$$

The following assumptions were used in the computational modeling: (1) the melted liquid flow in the middle annular region during the process appears to be transient, laminar, and incompressible; (2) the HTF temperature is constant in each case; (3) the PCM thermophysical properties remain constant throughout the range of involved case temperatures, and the PCM density is dominated by Boussinesq's hypothesis; (4) throughout the phase transition process of PCM, there is no volume variation, heat dissipation from the outer wall, and radiative heat transmission; and (5) at the boundary, there is no slip resulting from shear force.

2.3. Model validation

The geometry of this thermal energy storage system is straightforward, and its two-dimensional characteristics are prominent, thereby making the utilization of a 2D model for modeling and analysis a more efficient choice in terms of computational resource consumption. Previous researchers have also used this method for model simplification [43]. A 2D model, consistent with the previous investigations conducted by our research group, was implemented for simulation purposes [38]. The model simplifies the structures of the tube walls in contact with the PCM and replaces them with thermostatic boundary conditions. The grid employed in this paper is presented in Fig. 3. The computational grid utilized in this study is illustrated in Fig. 3 and comprises a combination of quadrilateral and triangular elements. Numerical simulation calculations were performed using Ansys fluent software, with the initial temperature state of the PCM set at 300 K.

The mesh independence validation as well as the model validation are the same as the previous work of our group [38]. The experimental data from Al-Abidi [44] were used for the grid independence validation, and simulations were carried out under the same working conditions as the experiments with the grid numbers 16,117, 49,908, and 80,258. The results of the simulations are shown in Fig. 4(a), which indicate that considering the number of grids in the model as well as the accuracy of the calculation, the final method of dividing the grid with the number of 49,908 has been chosen. The verification of time step independence is shown in Fig. 4(b). The influence of the three different time steps on the melting time is minimal. Ultimately, a time step of 0.3 s was determined to be the minimum.To ensure the accuracy of the model, it is necessary

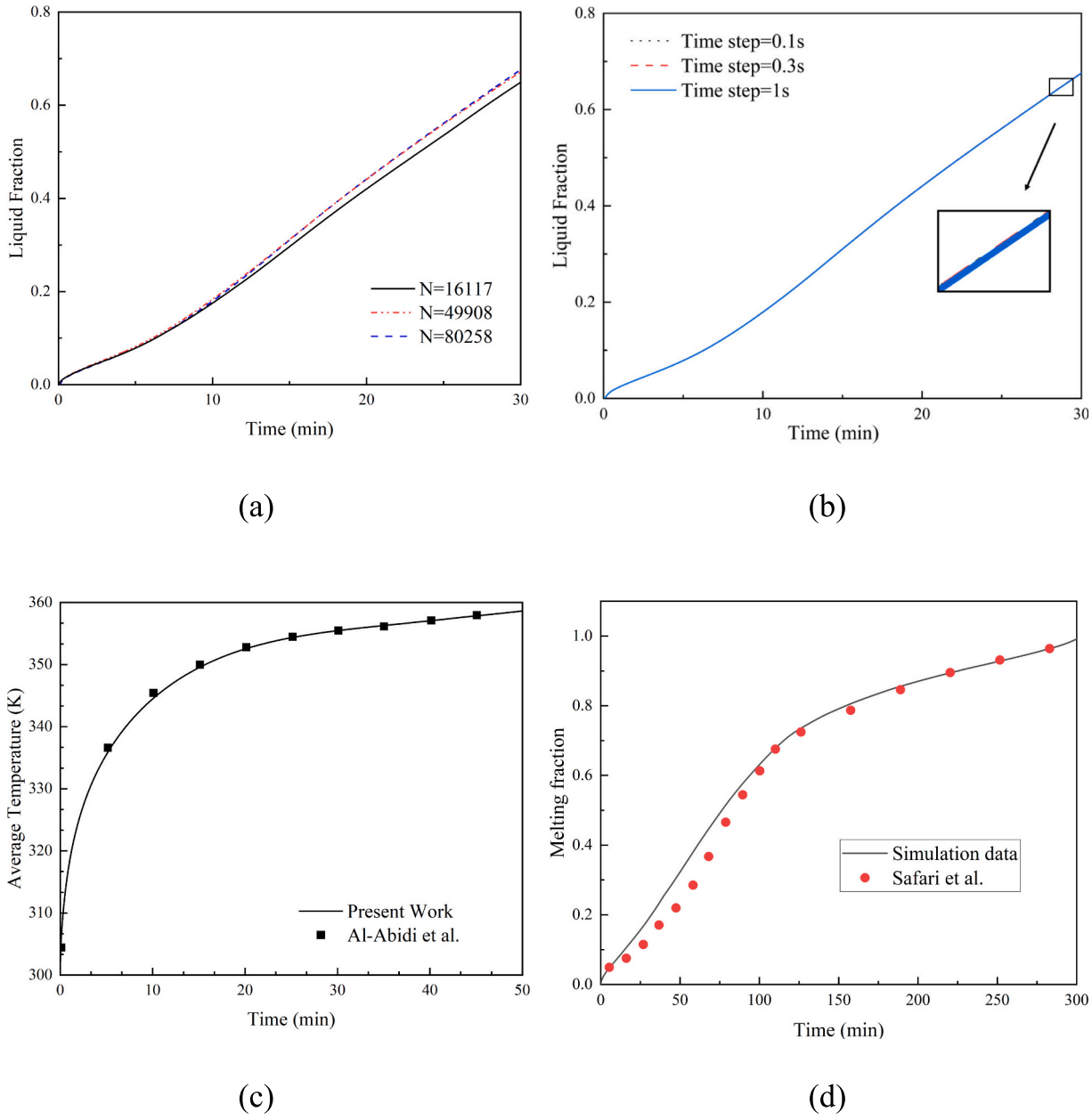

Fig. 4. Validation study (a) mesh independence validation; (b) model validation of melting temperature [38]; (c) model validation of melting fraction.

to validate the output results of different parameters [45]. The melting curves are analytically evaluated against the experimental data, and the information is shown in Fig. 4(c). In addition, the model is compared with experiments from Safari [46] under the same boundary conditions to validate the model melting fraction. Both of them demonstrate that the results are in good correlation and the numerical model used in this study matches well with the actual melting process.

3. Methods

3.1. Variable correlation analysis

Before performing machine learning training, the first step is to do correlation analysis of the variables. Correlation analysis is a type of scientific procedure used in examining the relevance of correlation between two or multiple random variables with the same state, when the correlation between the variables is high, it can be assumed that there is a hidden link between the variables, and in order to improve the predictive precision of a model, it is essential to simplify the input variables with high correlation. The assessment of correlation is usually achieved by calculating the Pearson correlation coefficient. The equation to calculate this coefficient r between variables j and k is

$$r_{j,k} = \frac{\sum_{i=1}^{n}[(j_i - \bar{j})\cdot(k_i - \bar{k})]}{\sqrt{\sum_{i=1}^{n}(j_i - \bar{j})^2}\cdot\sqrt{\sum_{i=1}^{n}(k_i - \bar{k})^2}} \tag{9}$$

It is usually concluded that when the absolute value of Pearson's correlation coefficient is less than 0.35 [47], two variables can be considered to show no correlation between them. The correlations were calculated separately for all the parameters and the results were plotted in the same matrix as shown in Fig. 5. The results of Pearson's correlation coefficient between any two parameters shown in the figure indicate that there is no significant correlation between the parameters.

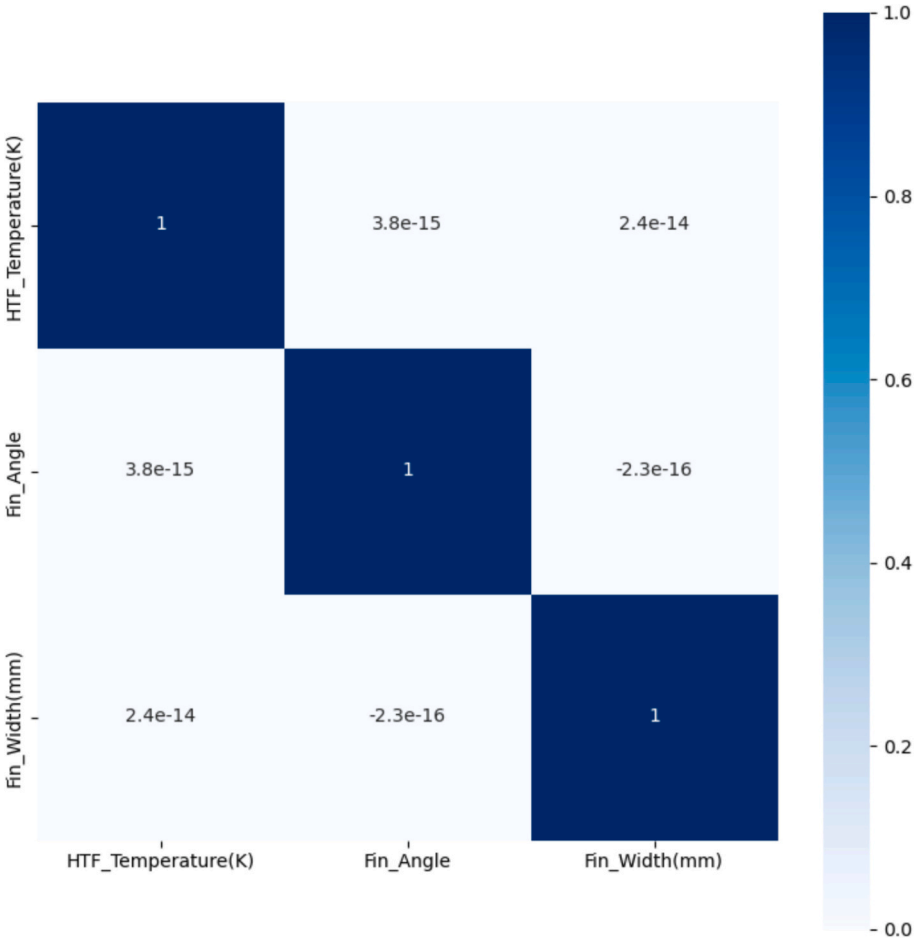

Fig. 5. Correlation matrix of parameters.

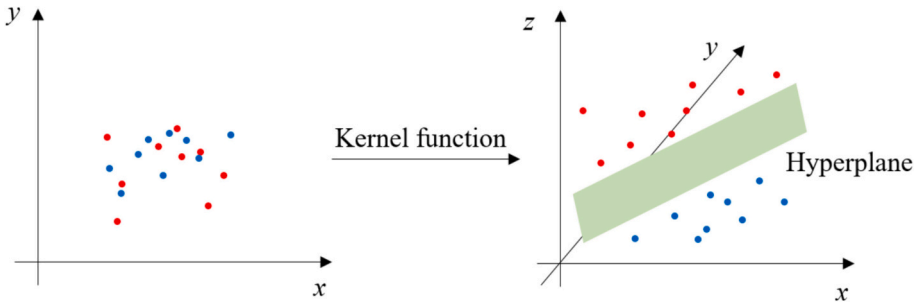

Fig. 6. Support vector machine algorithm.

3.2. Polynomial regression algorithm

The polynomial regression (PR) algorithm is based on the linear regression algorithm. The linear regression algorithm considers the relationship between the independent variables of the dataset and the objective to be linear, and is able to establish the loss function equation through the use of the least square method, and optimise the loss function through the gradient descent method. The polynomial regression algorithm is a method of pre-processing the features of established datasets by considering them as multidimensional features and then fitting them to a linear regression.

3.3. Support vector regression algorithm

As an algorithm with good robustness, the support vector regression (SVR) algorithm is an algorithm for linearly fitting data in a high-dimensional space through supervised learning, which was first proposed by Vapnik [48] and has become a popular machine learning algorithm. The implementation process is mainly divided into two steps. The first step is data upgrading, i.e., transforming the difficult-to-fit low-dimensional nonlinear data into high-dimensional linear data by a specific kernel function; the second step is hyperplane fitting, i.e., finding a regression plane to make all the data of a set to the nearest distance to the plane, and this hyperplane is the ideal hyperplane. Once the algorithm is trained, model result prediction can be achieved by simply mapping the new data to the high-dimensional space using the same method. The structure of the support vector regression algorithm is shown in Fig. 6.

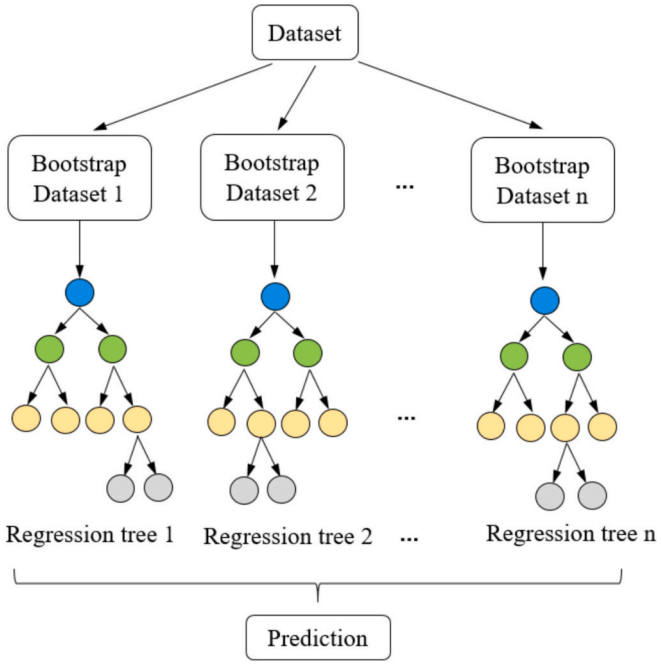

Fig. 7. Random forest regression algorithm.

3.4. Random forest algorithm

Integrated learning methods typically demonstrate high prediction accuracy. The random forest regression (RFR) algorithm [49] is an integrated learning algorithm that uses a large number of decision trees for regression prediction, aggregates the decision trees, and calculates the average of the outputs of each decision tree as the final regression prediction result. Because each sub-decision tree is from the same data set, it is inevitable that each decision tree will produce correlation, which will affect the prediction results, therefore, RFR uses two ieideologies to achieve tree de-correlation, which are the bagging ideology [50] and the random subspace ideology [51]. The structure of the RFR model is shown in Fig. 7.

3.5. XGBoost algorithm

As an integrated learning method, the extreme gradient boosting (XGBoost) [52] is a highly scalable gradient boosting algorithm based on decision trees. XGBoost is based on the concept of gradient boosting and generates decision trees separately and sequentially, where each tree learns from the residues of all the previous trees. Finally, the output predictions of these trees are aggregated to give the prediction result. The XGBoost algorithm avoids overfitting by integrating a regularisation term in the modeling process. The XGBoost algorithm has been schematically illustrated in Fig. 8.

3.6. Hyperparameter

There are two types of parameters in the training process of supervised machine learning algorithms, one can be obtained iteratively from the training process and is called the model parameter, while the other tuning parameter cannot be obtained iteratively and needs to be set manually by hand, which is called the hyperparameter. After these years of advancement of machine learning algorithms, researchers have come up with certain default values after empirical experiments on various datasets. The default values have no theoretical roots and are derived merely from experimental experience. In order to obtain better models, optimisation tuning strategies regarding predictive performance can be employed to select the values that are most suitable for the dataset under study.

3.7. Bayesian optimisation algorithm

Traditional optimisation algorithms, such as grid search, are computationally intensive and inefficient, making optimisation algorithms that can improve efficiency the preferred choice of researchers. The Bayesian optimisation algorithm is a global search algorithm that is able to exploit prior knowledge [53]. The core idea of the Bayesian optimisation algorithm is to generate an initial set of candidate sample solutions for the function to be optimised, then assume a priori distribution and continuously add candidate solutions, which are judged by a given scoring function to determine whether the candidate solutions are reasonable or not, and finally output the global maximum point of the candidate solutions after repeated iterations. It is an optimisation algorithm with relatively low computational overhead.

3.8. Model assessment

The dataset in this study with a capacity of 60 was segmented, where 70 % of the data point was partitioned into the training set, and the remaining 30 % of the data point was partitioned into the test set. This dataset is a full factorial dataset. A 3-fold cross-validation was adopted in the evaluation and the reason for not choosing more folds was due to the limit size of the dataset. Prediction models obtained by different machine learning algorithms need to be evaluated using the same quantitative metrics. There are two indicators called mean square error (MSE) as well as the coefficient of determination (R^2) were chosen to evaluate the results of machine learning models in this scenario.

MSE is the average of the summation of the squares of the targeted predicted data deviations from their actual values. Given that y_i represents the actual value which corresponds to the predicted value $h_i(x_i)$, the formula is

$$MSE = \frac{1}{n}\sum_{i=1}^{n}(h_i(x_i) - y_i)^2 \tag{10}$$

R^2 is the proportion of the dependent variable that could be explained by the regression relationship obtained by the fitted model for the target independent variable of a study. The model would have better interpretability if its R^2 close to 1. The coefficient of determination can

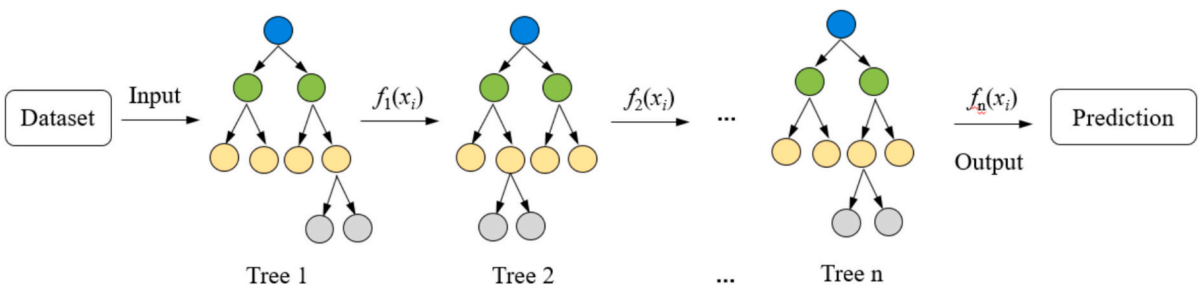

Fig. 8. XGBoost algorithm.

Table 3
Hyperparameter search spaces and chosen values.

Algorithm	Hyperparameter	Description	Search space	Value
PR	degree	polynomial dimension	[1,10]	2
SVR	gamma	coefficients of the kernel function	(0.0001,100)	0.154
	c	penalty factor	(0.1200)	186
	epsilon	regularisation parameter range	(0.0001,100)	0.369
RFR	n_estimators	tree number	[10,500]	65
	min_samples_leaf	samples minimum number required to be at a leaf node	[2,10]	2
	max_depth	maximum depth of trees	[2,10]	7
	min_samples_split	samples minimum number required to split an internal node	[2,5]	2
	max_features	number of variables to consider	[0.100,0.999]	0.999
XGboost	n_estimators	number of trees	[10,500]	497
	subsample	the training instances subsample ratio	[0.5,1)	0.933
	max_depth	maximum depth of trees	[2,10]	46
	min_child_weight	instance weight minimum sum needed in a child	[1,8]	2
	reg_alpha	L1 regularisation term on weights	(0,1)	0.768
	reg_lambda	L2 regularisation term on weights	(0,1)	0.529
	learning_rate	Step reduction used for updates	(0,0.5]	0.389
	gamma	minimum loss reduction required to make a further partition on a leaf node	(0,1)	0.544
	colsample_bytree	subsample ratio of columns when constructing each tree	[0.5,1]	0.908

be calculated as

$$R^2 = 1 - \frac{\sum_{i=1}^{n}(y_i - h_i(x_i))^2}{\sum_{i=1}^{n}(y_i - \overline{y}_i)^2} \tag{11}$$

4. Results and discussions

The numerical simulation results from the dataset employed in this study have been previously presented in the previous paper [38]; therefore, this paper will specifically concentrate on the results of the meta-models. The quantitative prediction results of this study do not separately summarize the effects of variables on melting time using the control variable method. Instead, they are aggregated within scatter plots to facilitate the observation of the reliability of the meta-model.

4.1. Hyperparameter tuning

The principles of each machine learning algorithm are different, and each algorithm weighs the efficiency of finding the global optimal solution and the optimal model fitting to achieve the minimised deviation from the expected value in a different way. As a result, the numbers of key hyperparameters and their meanings vary from one algorithm to another. In this study, the hyperparameter tuning of all four machine learning algorithms is accomplished based on the Bayesian optimisation algorithm. The scoring metrics for the optimisation results are chosen to be R^2 values, and hyper-parameters (e.g., the number of decision trees, etc.) for which the value needs to be an integer value during the iteration process are already rounded. The search intervals for each hyperparameter are given empirically. The hyperparameters that need to be rounded are already rounded during the tuning process. The final hyperparameters are taken to three significant digits to ensure that the results are sufficiently accurate. For each algorithm, the interpretation of each hyperparameter, the search space, and the final selected values are shown in Table 3. The PR algorithm has only one hyperparameter, so a manual tuning method was chosen, and the selected final values of the hyperparameters for each of the remaining algorithms were obtained by iterating the Bayesian algorithm for 400 steps, where the first 200 steps of the iteration are random searches within the hyperparameter candidate range, and the last 200 steps of the iteration are fine searches near the optimum of the previous 200 steps. This study implements all machine learning algorithms in the environment of Python 3.9, and all machine learning experiments were performed on a PC equipped with Intel (R) Core (TM) i5-8300H (@ 2.30 GHz), 24 GB of RAM, and running the Windows 11 operating system.

4.2. Algorithms performance analysis

The physical model parameters are treated as independent variables, with the melting response time as the dependent variable, establishing a nonlinear mapping. The four machine learning algorithms previously described are then employed to identify the algorithm that achieves the highest accuracy in this context. Using the hyperparameters obtained from the search in Section 4.1, the melting response time of the triplex-tube PCM-TES system was predicted with each algorithm, and the predicted results were compared with the actual results, as presented in Fig. 9. The predictions of the training set as well as the test set are labelled in Fig. 9, and the scatter points fall on the labelled auxiliary dotted lines when the predicted values are exactly the same as the actual values. From Fig. 9, it can be found that among the four algorithms, the algorithm with the largest deviation between the training set and the test set results is the SVR algorithm, which means that there is an obvious overfitting phenomenon, while the test set and the training set of the other algorithms have roughly the same distribution on both sides of the auxiliary line. The RF algorithm has the largest deviation, especially in the region of higher values, which indicates that its prediction accuracy is insufficient. The best performing algorithm was XGboost, whose data were able to be distributed roughly precisely around the auxiliary line.

The residual plots of the prediction results of the four algorithms are presented in Fig. 10. The results indicate that the residual value of the prediction results of the random forest algorithm is significantly higher than the other algorithms, and the maximum error of its prediction value is more than 15 min, and more results of high prediction value occur when the actual value is lower, while more results of low prediction value occur in the region of higher actual value. Both PR algorithm as well as SVR algorithm showed the prediction error close to 15 min for individual conditions, and the prediction accuracy of XGBoost algorithm was higher than the other algorithms, and its maximum error was approximately 5 min. With the exception of the RFR algorithm, the residuals of the test set for the other algorithms are larger than the training set residuals, which corresponds to the results in Fig. 9.

The prediction results were analyzed using the evaluation metrics presented in the previous section. The results of the mean square error comparison are presented in Fig. 11 (a), which can show that the data fitting quality of the training set is higher than that of the prediction set in general. The algorithm with the largest MSE gap is the SVR algorithm, which has an 11.8 times MSE gap in its predictions, indicating that the algorithm is overfitting more severely, meanwhile the PR algorithm is the best in terms of unbiasedness, which has an MSE difference of only 1.15 times. From the perspective of the absolute error of the test set, XGboost is the optimal algorithm, although the MSE of its test set differs from that of the training set by about 4.84 times. The coefficient of

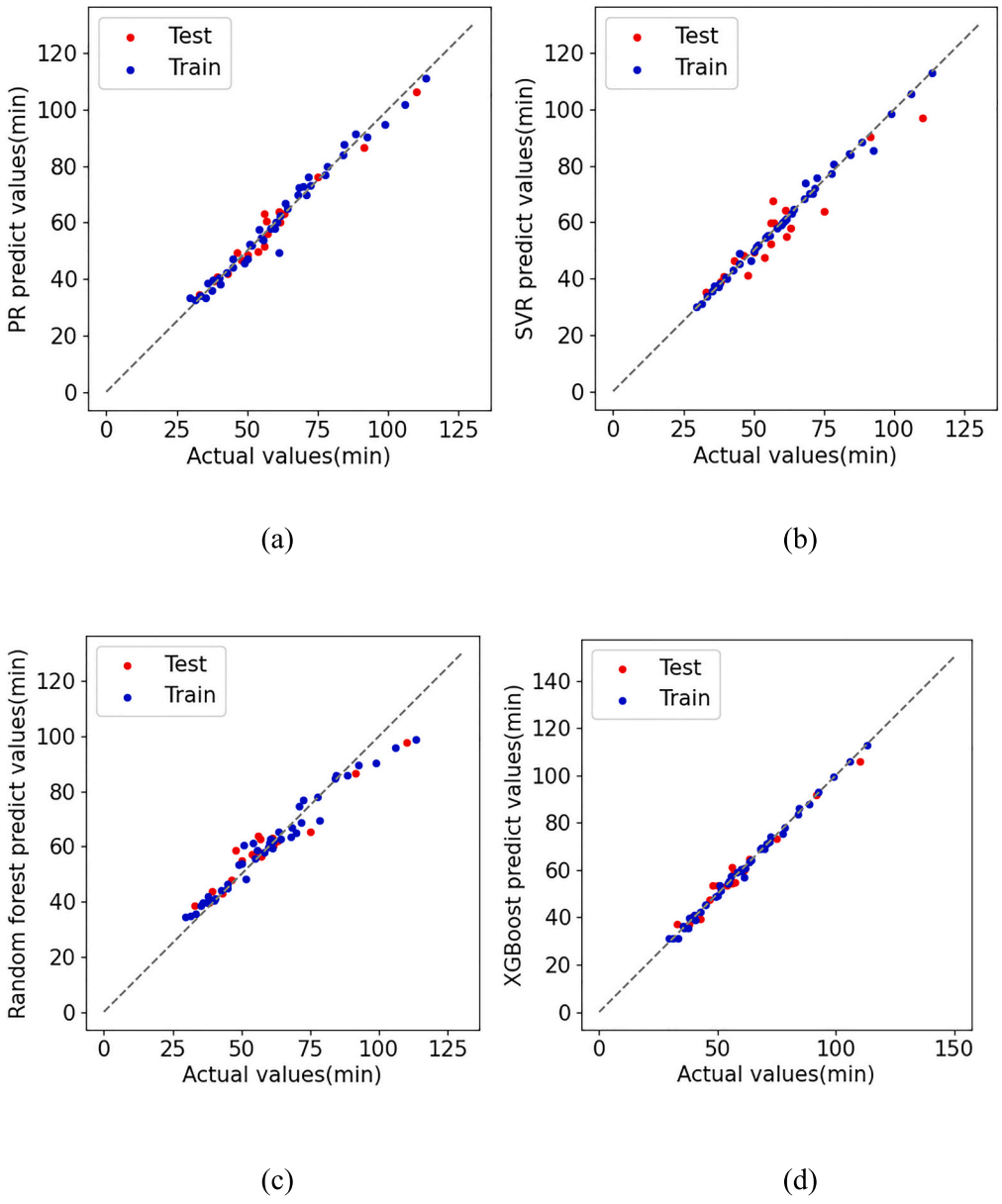

Fig. 9. PCM melting response time model prediction result reaped by (a) PR (b)SVR(*c*)RF(d) XGboost.

determination metrics presented in Fig. 11(b) exhibit similar findings, with the SVR algorithm having the lowest coefficient of determination for test set prediction results while the XGboost algorithm has the highest coefficient of determination for test set prediction results.

4.3. Feature importance evaluation

While traditional prediction methods such as empirical formulae can only qualitatively analyse the extent to which each parameter affects the melting response time, data-driven machine learning methods are able to quantitatively give this value directly and guide the subsequent design of the fin structure. The principle is to calculate the increase in model prediction error after substitution of features to measure the importance of the features. In this section, the importance of each parameter is evaluated. The predictions in this section are given based on the best-performing XGBoost algorithm. From the previous studies, it can be judged that both fin width and HTF temperature have a greater influence on the final melt rate, and from Fig. 12, it can be found that the importance of fin width is 51 % while the importance of HTF temperature is 47 %. This indicates that the increase in fin heat transfer area contributes the most to the enhanced heat transfer. The change in fin angle has a lesser effect on the melting response time with only 2 % importance. This suggests that changes in fin structure style have a small effect on heat transfer performance, and subsequent research should focus more on how to increase the surface area of the fins at a low cost with a fixed fin cross-section area.

After all, when an algorithm is deemed 'optimal' in a study, it is usually within the context of that specific research framework. This benchmarking establishes a baseline for future work, enabling researchers to identify which algorithms merit further exploration under similar conditions. Additionally, current machine learning research increasingly emphasizes generalization and transfer learning—applying knowledge gained in one domain to another. Insights into the superior performance of XGBoost in a specific configuration can inspire adaptations and modifications for different TES systems.

Although different types of PCMs or system configurations may lead to certain variations, the study demonstrates that machine learning algorithms maintain comparable accuracy across datasets with similar

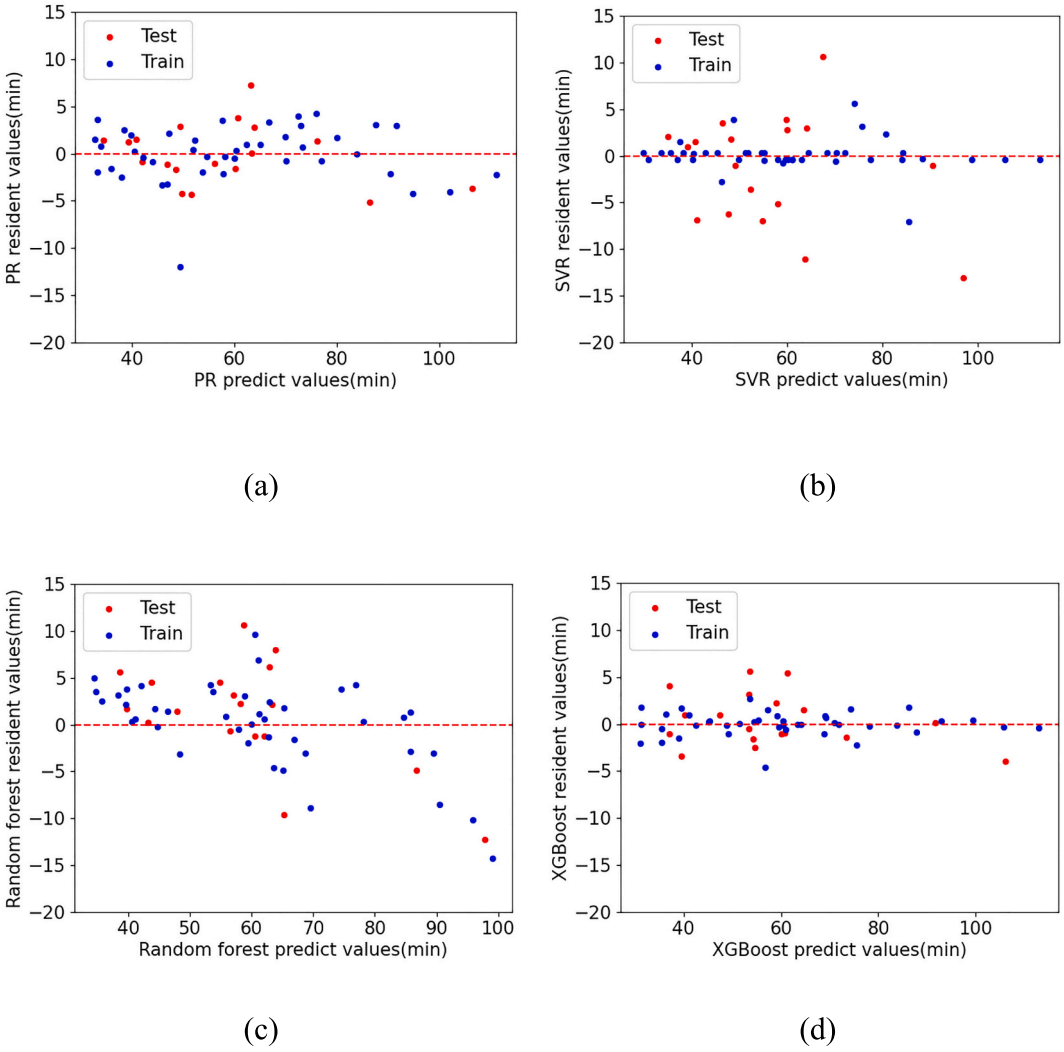

Fig. 10. PCM melting response time prediction residual errors of (a) PR (b)SVR(c)RF(d) XGboost.

structural characteristics. The performance of these models is primarily influenced by the statistical properties of the dataset rather than the specific physical attributes of the materials. Datasets with analogous patterns, irrespective of material variations, tend to yield consistent algorithmic outcomes. While the trained models may not be directly transferable to entirely distinct configurations, the meta-model selection approach remains consistent. The adoption of algorithms, which perform well across datasets with similar distributions, ensures robust model selection, even in the presence of PCM or configuration variations. Thus, while dataset diversity can impact prediction accuracy, the overall framework for similar systems remains reliable [54].

Moreover, the scalability of the algorithm is advantageous. In analogous scenarios, the model can be efficiently retrained by incorporating a small amount of additional data, making it adaptable to new datasets without necessitating a complete retraining process. This flexibility enhances the model's efficiency, particularly when managing evolving or expanded datasets within the same operational context.

5. Conclusions

This study explores the potential of machine learning-based meta-models in predicting the melting response time of phase change materials in triplex-tube latent thermal energy storage systems. By applying algorithms such as polynomial regression, support vector regression, random forest regression, and XGBoost, we constructed efficient predictive models that effectively replace traditional experimental and numerical methods.

The results show that the XGBoost algorithm outperforms others, achieving the highest accuracy and lowest prediction error. In contrast, support vector regression exhibits significant overfitting in the testing set, highlighting the need for appropriate meta-models to ensure reliable predictions. Sensitivity analysis based on XGBoost identifies key factors influencing melting response time, with fin width and heat transfer fluid temperature contributing 51 % and 47 %, respectively, while the fin angle has a minor effect at 2 %. These findings guide future design efforts, emphasizing the optimization of fin design to enhance heat

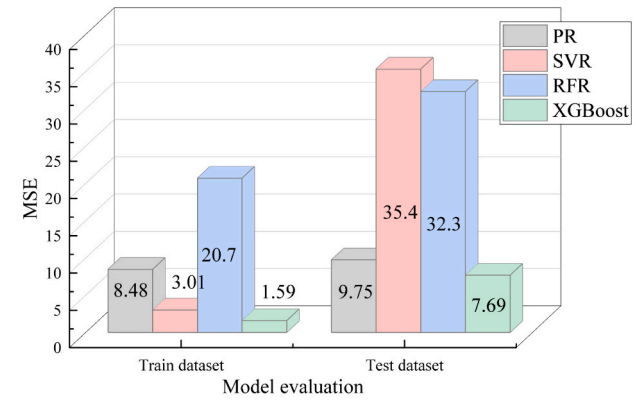

(a)

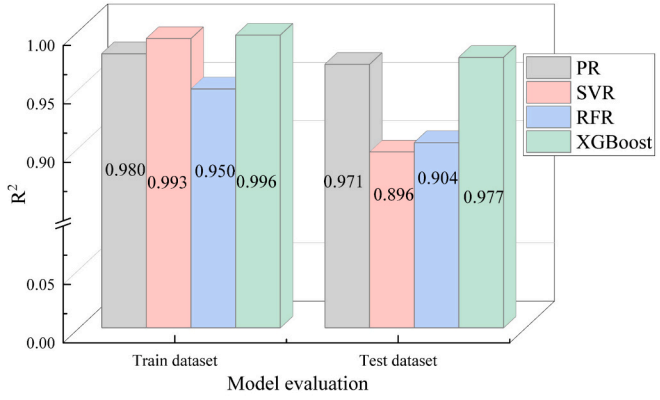

(b)

Fig. 11. The assessment scores for the four algorithm (a) MSE (b)R^2.

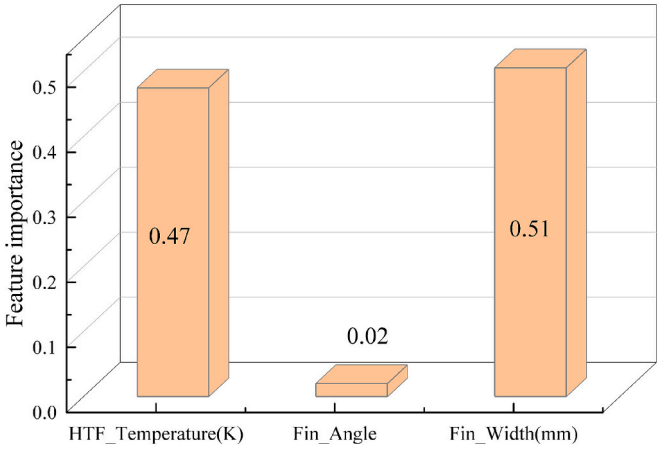

Fig. 12. Feature importance evaluation.

transfer efficiency. Machine learning-based meta-models hold great promise for the design and optimization of latent thermal energy storage systems, improving prediction accuracy and providing data-driven support for engineering decisions.

CRediT authorship contribution statement

Peiliang Yan: Writing – original draft, Methodology, Formal analysis, Conceptualization. **Chuang Wen:** Writing – review & editing, Supervision, Methodology, Formal analysis, Conceptualization. **Hongbing Ding:** Writing – review & editing, Methodology, Formal analysis. **Xuehui Wang:** Writing – review & editing, Formal analysis. **Yan Yang:** Writing – review & editing, Supervision, Methodology, Investigation, Formal analysis, Conceptualization.

Declaration of competing interest

The authors declare that they have no known competing financial interests or personal relationships that could have appeared to influence the work reported in this paper.

Data availability

Data will be made available on request.

References

[1] IPCC. Climate change 2023 synthesis report. 2023.
[2] Pouresmaieli M, Ataei M, Nouri Qarahasanlou A, Barabadi A. Integration of renewable energy and sustainable development with strategic planning in the mining industry. Results Eng 2023;20:101412.
[3] Hassan AA, El-Rayes K. Optimal use of renewable energy technologies during building schematic design phase. Appl Energy 2024;353:122006.
[4] Chen X, Xi X, Zhang L, Wang Z, Cui Z, Long W. Experimental study on nucleation and micro-explosion characteristics of emulsified heavy fuel oil droplets at elevated temperatures during evaporation. Appl Therm Eng 2023;224:120114.
[5] Abu-Hamdeh NH, Khoshaim A, Alzahrani MA, Hatamleh RI. Study of the flat plate solar collector's efficiency for sustainable and renewable energy management in a building by a phase change material: containing paraffin-wax/graphene and paraffin-wax/graphene oxide carbon-based fluids. J Build Eng 2022;57:104804.
[6] Mahdi JM, Nsofor EC. Melting enhancement in triplex-tube latent heat energy storage system using nanoparticles-metal foam combination. Appl Energy 2017;191:22–34.
[7] Yan P, Fan W, Han Y, Ding H, Wen C, Elbarghthi AFA, et al. Leaf-vein bionic fin configurations for enhanced thermal energy storage performance of phase change materials in smart heating and cooling systems. Appl Energy 2023;346:121352.
[8] Jain S, Kumar KR, Rakshit D. Heat transfer augmentation in single and multiple (cascade) phase change materials based thermal energy storage: research progress, challenges, and recommendations. Sustain Energy Technol Assess 2021;48:101633.
[9] Abilkhassenova Z, Memon SA, Ahmad A, Saurbayeva A, Kim J. Utilizing the Fanger thermal comfort model to evaluate the thermal, energy, economic, and environmental performance of PCM-integrated buildings in various climate zones worldwide. Energ Build 2023;297:113479.
[10] Choure BK, Alam T, Kumar R. A review on heat transfer enhancement techniques for PCM based thermal energy storage system. J Energy Storage 2023;72:108161.
[11] Sarkar S, Mestry S, Mhaske ST. Developments in phase change material (PCM) doped energy efficient polyurethane (PU) foam for perishable food cold-storage applications: a review. J Energy Storage 2022;50:104620.
[12] Khan MM, Alkhedher M, Ramadan M, Ghazal M. Hybrid PCM-based thermal management for lithium-ion batteries: trends and challenges. J Energy Storage 2023;73:108775.
[13] Du K, Calautit J, Eames P, Wu Y. A state-of-the-art review of the application of phase change materials (PCM) in mobilized-thermal energy storage (M-TES) for recovering low-temperature industrial waste heat (IWH) for distributed heat supply. Renew Energy 2021;168:1040–57.
[14] Goel V, Dwivedi A, Kumar R, Kumar R, Pandey AK, Chopra K, et al. PCM-assisted energy storage systems for solar-thermal applications: review of the associated problems and their mitigation strategies. J Energy Storage 2023;69:107912.
[15] Li S, Zou K, Sun G, Zhang X. Simulation research on the dynamic thermal performance of a novel triple-glazed window filled with PCM. Sustain Cities Soc 2018;40:266–73.
[16] Agarwal P, Prabhakar A. Energy and thermo-economic analysis of PCM integrated brick in composite climatic condition of Jaipur - a numerical study. Sustain Cities Soc 2023;88:104294.
[17] Zavrl E, Tomc U, El Mankibi M, Dovjak M, Stritih U. Parametric study of an active-passive system for cooling application in buildings improved with free cooling for enhanced solidification. Sustain Cities Soc 2023;99:104960.
[18] Al-Abidi AA, Bin Mat S, Sopian K, Sulaiman MY, Lim CH, Th A. Review of thermal energy storage for air conditioning systems. Renew Sust Energ Rev 2012;16:5802–19.
[19] Xu B, Lu S, Zheng J. Thermodynamic optimization of cascaded PCMs charge process based on entransy dissipation extreme principle. Sustain Cities Soc 2023;93:104521.

[20] Palmer B, Arshad A, Yang Y, Wen C. Energy storage performance improvement of phase change materials-based triplex-tube heat exchanger (TTHX) using liquid–solid interface-informed fin configurations. Appl Energy 2023;333.
[21] Nitsas M, Koronaki IP. Performance analysis of nanoparticles-enhanced PCM: an experimental approach. Thermal Sci Eng Progress 2021;25:100963.
[22] Saraf SD, Panda D, Gangawane KM. Performance analysis of hybrid expanded graphite-NiFe2O4 nanoparticles-enhanced eutectic PCM for thermal energy storage. J Energy Storage 2023;73:109188.
[23] Huang X, Yao S, Yang X, Zhou R, Luo J, Shen X. Comparison of solidification performance enhancement strategies for a triplex-tube thermal energy storage system. Appl Therm Eng 2022;204:117997.
[24] Huang X, Yao S, Yang X, Zhou R. Melting performance assessments on a triplex-tube thermal energy storage system: optimization based on response surface method with natural convection. Renew Energy 2022;188:890–910.
[25] Liu J, Liu Z, Nie C. Phase transition enhancement through circumferentially arranging multiple phase change materials in a concentric tube. J Energy Storage 2021;40:102672.
[26] Al-Abidi AA, Mat S, Sopian K, Sulaiman MY, Mohammad AT. Numerical study of PCM solidification in a triplex tube heat exchanger with internal and external fins. Int J Heat Mass Transf 2013;61:684–95.
[27] Zonouzi SA, Dadvar A. Numerical investigation of using helical fins for the enhancement of the charging process of a latent heat thermal energy storage system. J Energy Storage 2022;49:104157.
[28] Rieger H, Projahn U, Beer H. Analysis of the heat transport mechanisms during melting around a horizontal circular cylinder. Int J Heat Mass Transf 1982;25:137–47.
[29] Wang Y, Amiri A, Vafai K. An experimental investigation of the melting process in a rectangular enclosure. Int J Heat Mass Transf 1999;42:3659–72.
[30] Assis E, Katsman L, Ziskind G, Letan R. Numerical and experimental study of melting in a spherical shell. Int J Heat Mass Transf 2007;50:1790–804.
[31] Chabot C, Gosselin L. Solid-liquid phase change around a tube with periodic heating and cooling: scale analysis, numerical simulations and correlations. Int J Therm Sci 2017;112:345–57.
[32] Cai J, Xu K, Zhu Y, Hu F, Li L. Prediction and analysis of net ecosystem carbon exchange based on gradient boosting regression and random forest. Appl Energy 2020;262:114566.
[33] Yan P, Fan W, Zhang R. Predicting the NOx emissions of low heat value gas rich-quench-lean combustor via three integrated learning algorithms with Bayesian optimization. Energy 2023;273:127227.
[34] Wallimann H, Sticher S. On suspicious tracks: machine-learning based approaches to detect cartels in railway-infrastructure procurement. Transp Policy 2023;143:121–31.
[35] Ermis K, Erek A, Dincer I. Heat transfer analysis of phase change process in a finned-tube thermal energy storage system using artificial neural network. Int J Heat Mass Transf 2007;50:3163–75.
[36] Fini AT, Fattahi A, Musavi S. Machine learning prediction and multiobjective optimization for cooling enhancement of a plate battery using the chaotic water-microencapsulated PCM fluid flows. J Taiwan Inst Chem Eng 2023;148.
[37] Chuttar A, Banerjee D. Machine learning (ML) based thermal Management for Cooling of electronics chips by utilizing thermal energy storage (TES) in packaging that leverages phase change materials (PCM). Electronics 2021;10:2785.
[38] Yan P, Fan W, Yang Y, Ding H, Arshad A, Wen C. Performance enhancement of phase change materials in triplex-tube latent heat energy storage system using novel fin configurations. Appl Energy 2022;327:120064.
[39] Ye W-B, Arıcı M. False diffusion, asymmetrical interface, and equilibrious state for pure solid-gallium phase change modeling by enthalpy-porosity methodology. Int Commun Heat Mass Transfer 2023;144:106746.
[40] Brent AD, Voller VR, Reid KJ. Enthalpy-porosity technique for modeling convection-diffusion phase change: application to the melting of a pure metal. Numerical Heat Transfer 1988;13:297–318.
[41] Hameter M, Walter H. Influence of the mushy zone constant on the numerical simulation of the melting and solidification process of phase change materials. Comput Aided Chem Eng 2016;38:439–44.
[42] Ye W-B, Arıcı M. Exploring mushy zone constant in enthalpy-porosity methodology for accurate modeling convection-diffusion solid-liquid phase change of calcium chloride hexahydrate. Int Commun Heat Mass Transfer 2024;152:107294.
[43] Ye W-B, Arıcı M. 3D validation, 2D feasibility, corrected and developed correlations for pure solid-gallium phase change modeling by enthalpy-porosity methodology. Int Commun Heat Mass Transfer 2023;144:106780.
[44] Al-Abidi AA, Mat S, Sopian K, Sulaiman MY, Mohammad AT. Experimental study of melting and solidification of PCM in a triplex tube heat exchanger with fins. Energ Build 2014;68:33–41.
[45] Ye W-B, Arıcı M. Redefined interface error, 2D verification and validation for pure solid-gallium phase change modeling by enthalpy-porosity methodology. Int Commun Heat Mass Transfer 2023;147:106952.
[46] Safari V, Abolghasemi H, Darvishvand L, Kamkari B. Thermal performance investigation of concentric and eccentric shell and tube heat exchangers with different fin configurations containing phase change material. J Energy Storage 2021;37:102458.
[47] Taylor R. Interpretation of the correlation coefficient: a basic review. J Diagnostic Med Sonography 1990;6:35–9.
[48] Cortes C, Vapnik V. Support-vector networks. Mach Learn 1995;20:273–97.
[49] Breiman L. Random forests. Mach Learn 2001;45:5–32.
[50] Breiman L. Bagging predictors. Mach Learn 1996;24:123–40.
[51] Tin Kam H. The random subspace method for constructing decision forests. IEEE Trans Pattern Anal Mach Intell 1998;20:832–44.
[52] Chen T, Guestrin C. XGBoost: A Scalable Tree Boosting System. Proceedings of the 22nd ACM SIGKDD International Conference on Knowledge Discovery and Data Mining: Association for Computing Machinery; 2016. p. 785–94, numpages = 10.
[53] Snoek J, Larochelle H, Adams RP. Practical Bayesian optimization of machine learning algorithms. Proceedings of the 25th International Conference on Neural Information Processing Systems - Volume 2. Lake Tahoe, Nevada: Curran Associates Inc.; 2012. p. 2951–9.
[54] Uddin S, Lu H. Dataset meta-level and statistical features affect machine learning performance. Sci Rep 2024:14.